INDIAN JOURNAL OF SCIENCE AND TECHNOLOGY

RESEARCH ARTICLE

Optimization of Facial Images to Predict Gender Using HDSON and Bidirectional Associative Memory

Shoba Rani Salvadi[1]*, D Nagendra Rao[2], S Vathsal[3]

1 Research scholar, Jawaharlal Nehru Technological University, Hyderabad, Telangana, India
2 Professor and Principal, Abhinav-Hitech College of Engineering, Moinabad, Telangana, India
3 Retired DRDO Scientist

OPEN ACCESS

Received: 26-12-2022
Accepted: 03-02-2023
Published: 02-05-2023

Citation: Salvadi SR, Rao DN, Vathsal S (2023) Optimization of Facial Images to Predict Gender Using HDSON and Bidirectional Associative Memory . Indian Journal of Science and Technology 16(17): 1276-1283. https://doi.org/10.17485/IJST/v16i17.2481

* **Corresponding author**.

reddymallashobarani2@gmail.com

Funding: None

Competing Interests: None

Copyright: © 2023 Salvadi et al. This is an open access article distributed under the terms of the Creative Commons Attribution License, which permits unrestricted use, distribution, and reproduction in any medium, provided the original author and source are credited.

Published By Indian Society for Education and Environment (iSee)

ISSN
Print: 0974-6846
Electronic: 0974-5645

Abstract

Objective: To enhance the Gender prophecy by employing facial images using imaginative algorithm and to resolve real time applications. **Method:** Initially, we make use of shared deep octonion network and the Octonion-Valued Neural Network (OVNN) to develop a generic framework for a Hybrid Deep Sparse Octonion Network (HDSON). Sparse Coding Octonion data Algorithm (SCOA) is exploited to depict the face images up to seven color channels and improves the weight of HDSON. Furthermore, to take advantage of the maximum storage we make use of Bidirectional Associative Memories (BAM). **Findings:** The proposed approach resolves both the issues of depiction of the facial image and its storage, since the present study combines the characteristics of SCOA to improve HDSON weight and BAM to enhance the storage. Moreover, the present study is simple to apply and effective in real time applications. **Novelty:** The proposed approach can be used in paramilitary to minimize cross border terrorism; in addition, the presented scheme can enhance the probability of child detection and may help local police to a large extent.

Keywords: Automatic Gender Classification; BAM; DCN; HDSON; Octonion; SCOA; OVNN

1 Introduction

Technological developments in medical science grows rapidly; as a result, it becomes very complicated to identify the sex from facial image. So, to recognize the sex from facial image will become a vital problem and leads security issues. Consequently, this issue switches the attitude of signal and image processing researchers to exploit the problem; numerous theories and model have been developed to mitigate these issues. However, most approaches used complex image processing algorithms and make use neural networks to study the image performance and increases the delay thereby reduces the overall throughput.

Characteristics of the human face may be used to get information about a person's age, gender, emotional state, and ancestry[1,2]. Among these characteristics, age and gender recognition can be particularly useful, where gender must be determined by

their faces, but there are still various issues with age and gender credentials that pose open difficulties. Despite being state-of-the-art, predictions from unfiltered real life face photos have not yet met the demand for commercial and real time applications. Hence, it is crucial to have a reliable and precise system for age and gender identification, since this research focuses on gender prediction based on data collected and openly available datasets[3,4]. Ithas been stated that many different in real time neural network models have been built, as a whole[5], these models may be split into two classes: shallow and deep. Non-deep models are typically built using a multilayer perceptionmodule, which makes training challenging with the real-valued back propagation (BP) technique. One can roughly build deep models using pretrained methods like deep belief nets[6,7], deep auto-encoder[8], LeNet-5, Alex Net, Inception etc.[9].

Real Convolution neural network (RCNN) has widespread success in various applications, however correlations between convolution kernels are rarely considered, and i.e., no specific link or connection is created among convolution kernels. Moreover, real-value recurrent neural networks (Real RNNs) acquire the correlations by connecting and learning the weights of convolution kernels and the training difficulty is much increased.

Moumen et al[10] used Complex algebra and quaternion algebra to increase performance during model the connections between convolution kernels. Subsequently, lot of effort is required to design neural networks to work in the complex, quaternion, and octonion spaces, which are outside the existing domain. In[11] a deep learning model is used to determine a gender based on photographs of their retinas. In these approach authors used multiple stored images to train the model. However, to predict a person's gender based on the image requires a good explanatory power, which is not currently available, since the doctors currently have lack of information about gender-specific differences in retinal features. It is possible that the suggested deep learning may allow for the automatic discovery of new images and illness biomarkers under the direction of clinicians. In [12,13]authors discussed how age and gender can be determined using CNN, cell phone and machine learning technologies, however the authors need strong CNN to be available in the cell phone which may not be optimum with the currently available hardware. Katna et al[14] used machine learning to identify gender. The suggested technique achieved an accuracy of 81.2% for gender prediction. Various approaches[15–17] based on octonion-valued neural network (OVNN) have been presented to investigate the image property. The two approaches run on static data, hence may not be the optimum solution for real time application. Xiao et al[18] introduces fractional-order octonion-valued bidirectional attention mechanism. The system is too complex and reduced the overall throughput of the system.

In this paper an enhanced algorithm called hybrid of HDSON and Bidirectional Associative Memory Model(HHBM). In this approach we make use of HDSON to consider the facial image and BAM to improve the storage capacity of the system.Consequently, a hybrid model is developed having both the properties of HDSON and BAM and improves the performance of the existing systems[15–17].

The rest of the paper is organized as follows, in section 2 we are presenting our proposed model, section 3 presents results and discussion and finally we are concluding our paper in section 4.

1.1 Proposed Model

The proposed model presented has the following folds.

- **Sparse coding step:** The complex and quaternionsparse coding difficulties are generalizations of the problem posed in[19]. After multiplication, the generated matrix is represented in Table 1 having orthogonal columns. The study acquired a structured coefficient matrix to maintain the orthogonality property and the correlation between spectral channels. Contemporary, it can still rely on the tried-and-true linear correlation method across color channels to keep colors accurate. Compared to the standard concatenation model, this method enhanced connection between the image channels. It has been observed that the '1-norm minimization issue for octonionic signals may be transformed into a genuine convex optimization problem. To minimize the issue modified OMP for the octonion settings is employed. The presented algorithm chooses the atom d_k at each step k that minimizes the residual $\left\|r^k\right\|_2^2 = \left\|r^{k-1} - d_k x_k\right\|_2^2$, where r $^0 = y$

In the context of an octonion, it has been proven that this is identical to picking the atom with the highest correlation with the residual vector $\left\langle r^k, d_k \right\rangle$. Explicitly, the active dictionary is created as $D^k = \left(D^{k-1}, d_k\right]$ by selecting the atom that yields the highest absolute value in the inner product with the residual. Where,$'x'$ is the coding coefficient to minimize the norm $\left\|y - D^k x\right\|_2^2$. The Octonion-based linear least-squares problems are hard to solve; therefore, the study employs a new technique that involves changing the minimization issue into a genuine vector minimization problem represented in[19] and can be represented as

$$\left\|y - D^k x\right\|_2^2 = \left\|v\left(y - D^k x\right)\right\|_2^2 = \left\|v(y) - \chi\left(\mathrm{D}^k\right)\mathrm{v(x)}\right\|_2^2 \quad (1)$$

Table 1. Rules of multiplication among basis elements

	1	e1	e5	e3	e4	e6	e7	e2
1	1	e1	e5	e3	e4	e6	e7	e2
e1	e1	−1	−e4	−e2	e5	−e7	e6	e3
e2	e2	−e3	e7	e1	−e7	−1	e2	−1
e3	e3	e2	−e6	−1	e7	e5	−e4	−e1
e4	e4	−e5	e1	−e3	e7	e1	e3	−e6
e5	e5	e4	−1	e6	−e1	−e3	e2	−e7
e6	e6	e7	e3	−e5	−e2	−1	−e1	e4
e7	e7	−e6	−e2	e4	−e3	e1	−1	e5

- **Bidirectional Associative Octonion-Valued Memories:** The bidirectional associative memory[20] is employed in unidirectional Hopfield neural networks (HNN) and in various applications of pattern recognition and automatic control. Here we use Bidirectional associative memories to store and solve optimization problems associated with octonion based algorithms and can be represented regarding equations as:

$$\begin{cases} \tau_i \dfrac{dx_i(t)}{dt} = -x_i(t) + \displaystyle\sum_{j=1}^{P} w_{ij} f\left(y_i(t)\right) + a_i, & \forall i \in \{1,\ldots,N\} \\ v_j \dfrac{dy_j(t)}{dt} = -y_i(t) + \displaystyle\sum_{i=1}^{N} w_{ji} f\left(x_i(t)\right) + b_j, & \forall j \in \{1,\ldots,P\} \end{cases} \tag{2}$$

Where,$\tau_i \in R, \tau_i > 0$ and $\upsilon_j \in R, \upsilon_j > 0$ signify the time coefficients of neurons x_i and y_j, Respectively, $x_i(t)$, $y_j(t) \in O$ are the conditions of neurons x_i and $y_i$at time t; correspondingly, $w_{ij}O$ is the weight connecting neuron x_i to octonion data and $\frac{dx_i(t)}{dt} := \sum_{a=0}^{7} \frac{d([x_i]a)}{dt} e_a$. The weights and activation function values are multiplied by the octonion multiplication in the above mentioned differential equations$Ui\,(t) = f(xi\,(t))$, $andV\,j\,(t) = f(yj\,(t))$ are the outputs of neurons $x_i$andy_j, correspondingly in the system.

- **Deep octonion networks:** Beneath the shadow of this network, several modules are presented, such as the batch normalization module, the convolution module and the octonion weight initialization technique [21,22]. Here we enhance these models by modifying the mathematical models to get optimized results of the image.
- **Octonion internal representation technique :** Instead of employing real numbers to signify an octonion number, it uses them to reproduce the operations of an octonion number and can be divided into 8 parts to generate an octonic illustration. If an octonic Convolutional includes N feature maps, each divisible by 8, then the actual portion receives the first N/8 feature maps, while the seven remaining N/8 are allocated to the seven parts described in Table 1 .
- **Octonion convolution component:** the octonion convolution an Octonion vector is implemented by an octonion filter matrix and can be represented as

$$\begin{vmatrix} R(w_{0*0}x_0) \\ I(w_{0*0}x_0) \\ J(w_{0*0}x_0) \\ K(w_{0*0}x_0) \\ E(w_{0*0}x_0) \\ L(w_{0*0}x_0) \\ M(w_{0*0}x_0) \\ N(w_{0*0}x_0) \end{vmatrix} = \begin{bmatrix} w_0 & -w_1 & -w_2 & -w_3 & -w_4 & -w_5 & -w_6 & -w_7 \\ w_1 & w_0 & -w_3 & w_2 & -w_5 & w_4 & w_7 & -w_6 \\ w_2 & w_3 & w_0 & -w_1 & -w_6 & -w_7 & w_4 & w_5 \\ w_3 & w_2 & w_1 & w_0 & -w_7 & w_6 & -w_5 & w_4 \\ w_4 & w_5 & w_6 & w_7 & w_0 & -w_1 & -w_2 & -w_3 \\ w_5 & -w_4 & w_7 & -w_6 & w_1 & w_0 & w_3 & -w_2 \\ w_6 & -w_7 & -w_4 & w_5 & w_2 & -w_3 & w_0 & w_1 \\ w_7 & w_6 & -w_5 & -w_4 & w_3 & w_2 & -w_1 & w_0 \end{bmatrix} * \begin{bmatrix} x_0 \\ x_1 \\ x_2 \\ x_3 \\ x_4 \\ x_5 \\ x_6 \\ x_7 \end{bmatrix} \tag{3}$$

Octonion and real convolution are denoted by the symbols $*_0$ and$*$. All the numbers in the range $1, 2, \ldots, 7$ are represented by $x_i and w_i$, where i is a positive integer. The real component of $\bullet$ is denoted by the symbol $R(\bullet)$ where each of the seven imaginary portions is denoted by a letter of the alphabet. If a real-valued convolution is used, each channel is multiplied in the kernel by the

same number as in the input image. Finally, one feature map is generated using 8 kernels to concatenate 8 channels, followed by adding the resulting data to the prior operation's result. For each feature map, octonic convolution employs eight convolution kernels, utilizing the octonion arithmetic rule and follows the preceding process of 1×1 convolution.

- **Octonion batch normalization unit:** This improves training speed of the network Real numbers are normalized by translating and scaling them to make mean and variance equal to zero while applied to batch normalization. However, in the case of complex or quaternion numbers, batch normalization doesn't guarantee equal alteration in both real and imaginary parts. Therefore, a whitening strategy is utilized to scale the information by principal component to minimize the gap and can be represented mathematically as:

$$\tilde{\chi} = \frac{(x - E[x])}{\sqrt{v}} V \tag{4}$$

Where

$$V = \begin{bmatrix} v_{rr} & v_{ri} & v_{rj} & v_{rk} & v_{re} & v_{rl} & v_{rm} & v_{rn} \\ v_{ir} & v_{ii} & v_{ij} & v_{ik} & v_{ie} & v_{il} & v_{im} & v_{in} \\ v_{jr} & v_{ji} & v_{jj} & v_{jk} & v_{je} & v_{jl} & v_{jm} & v_{jn} \\ v_{kr} & v_{ki} & v_{kj} & v_{kk} & v_{ke} & v_{kl} & v_{km} & v_{kn} \\ v_{er} & v_{ei} & v_{ej} & v_{ek} & v_{ee} & v_{el} & v_{em} & v_{en} \\ v_{lr} & v_{li} & v_{ij} & v_{lk} & v_{le} & v_{ll} & v_{lm} & v_{ln} \\ v_{mr} & v_{mi} & v_{mj} & v_{mk} & v_{me} & v_{ml} & v_{mm} & v_{mn} \\ v_{nr} & v_{ni} & v_{nj} & v_{nk} & v_{ne} & v_{nl} & v_{nm} & v_{nn} \end{bmatrix} \tag{5}$$

Moreover, the octonion batch normalization layer's forward conduction can be calculated as:

$$\text{Octonion } BN(\tilde{x}) = \gamma\tilde{x} + \beta \tag{6}$$

Where $\beta = E(x) \in O^8$ and $\gamma = \sqrt{V\varepsilon O^{8\times8}}$

- **Octonion weight initialization method:** Here in the network parameters are set to their default values before training. As the network will not be able to learn the features if the weights are set to the same value at the outset. This kind of initialization makes deeper useless for deep neural networks and gives results that are worse than linear classifiers. So, to guarantee a gap between input and output to facilitate the model's rapid and stable convergence. To achieve the desired goal we choose a set of starting weight values that are all distinct and close to 0. In light of this, we present a means of setting the initial value for the weight of an octonion. Suppose that the eight components of the octonion weight $W_o \in O^{N\times N}$ are independent Gaussian random variables with a zero mean and same variance to get the dispersion ofW_o.

$$Var(W_0) = E\left((W_0|^2\right] - E\left((W_0|^2\right] \tag{7}$$

Since the 8 parts are zero-mean then,$E[|W_0|] = 0$as they have the same variance, then$Var(W_0) = 8\sigma^2$. The value of the standard deviation σ can then be represented as:

$$\sigma = \begin{cases} \frac{1}{2\sqrt{n_{\text{in}} + n_{\text{out}}}}, & \text{if Glorot sinitialization} \\ \frac{2}{\sqrt{n_{in}}}, & \text{if He } ' \text{ Sinitialization} \end{cases} \tag{8}$$

Here, the weight W_o is optimized, which is described as follows. The input of the deep octonion network is also an input of OVNN to classify the solution for Eq. (8).

- **Octonion Valued Neural Network (OVNN):** It develops the octonion valued form of octonion statistics given like

$$O^{def} = x_1 + i_1 x_2 + i_2 x_3 + i_3 x_4 + i_4 x_5 + i_5 x_6 + i_6 x_7 + i_7 x_8 \tag{9}$$

Where: $x_i, i \in \{1,2,..,8\}$ Is the real part and can be represented as

$$x_1, x_2, x_3, x_4, x_5, x_6, x_7, x_8 \in R \tag{10}$$

And $i_j, j \in \{1,2,\ldots,7\}$is the imaginary part and is given as

$$= i_2^2 = i_3^2 = i_4^2 = i_5^2 = i_6^2 = i_7^2 = -1 \tag{11}$$

The latter consists of m neurons and an output layer with s neurons. Weights w_{nm}^1 andw_{nm}^2, in turn, are associated with these layers. Biases are denoted by w_{0m}^1 for the hidden layer and w_{0s}^1 for the output layer. Octonion refers to all possible configurations of the inputs and outputs in a network. Furthermore, the output of the jth in OVNN can be calculated as:

$$\widehat{y}_j(k+1) = f^2\left(\widetilde{y}_j^{Re}\right) + \sum_{r=1}^{7} i_r f^2(\widetilde{y}_j^{Im(i_r)}) \tag{12}$$

Where Re and $Im(i_r)$directories are imaginary parts of$i_1, i_2, i_3, i_4, i_5, i_6$, and$i_7$, respectively, f^2 is the nonlinear sigmoid function given by $f^2(.) = \frac{1}{1+e^{-(.)}}$ and $\widetilde{y} = \sum_{l=1}^{m} w_l^2 h_l + w_0^2$

Furthermore, the real-valued delta rule is expanded upon as follows to help find the best values for network characteristics like weights and bias and can be given by

$$w_{0s}^2 = w_{0s}^{2Re} + i_1 w_{0s}^{2Im(i_1)} + i_2 w_{0s}^{2Im(i_2)} \pm \cdots + i_7 w_{0s}^{2Im(i_7)} \tag{13}$$

So by the applications of the above discussion the modified approach is therefore given by

$$\nabla_{w_{nm}^1} E = \frac{\partial E}{\partial w_{nm}^{1Re}} + \sum_{r=1}^{7} i_r \frac{\partial E}{\partial w_{nm}^{1Im(i_r)}} \tag{14}$$

$$\nabla_{w_{nm}^1} E = -u_n^* . \nabla_{w_{nm}^1} E \tag{15}$$

$$w_{nm}^1(k+1) = w_{nm}^1(k) = -\eta \nabla_{w_{nm}^1} E \tag{16}$$

- **Models' configurations for Octonion input construction:** Using this approach it is possible to obtain seven imaginary parts of octonic matrices by simultaneously performing one real-valued residual block for gender prediction. The octonion matrix and the real part are the eight vectors linked together along a specific axis to create an entirely new type of vector called an "octonion." This process of Octonion Conv is used to condense the octonion input, and it is followed by the ReLU operation, where OctonionBN specifies a batch normalization of the octonion input. Figure 1 presents the architecture of the projected model.

There are now three stages in which the octonion output is fed. Multiple blocks with two convolution layers remain at each level. To ensure the expressiveness of the output features, the number of feature maps is steadily raised in all three stages. Next, an AveragePooling2D layer is used to speed up training, and then a fully connected layer named Dense is used to classify the data. There are three blocks in the deep octonion network model. The first block has a total of 10 residual blocks, the second has 9 convolution filters, and the final blocks have 32, 64, and 128 residual blocks. The batch size has been set at 64. Table 2 provides the learning rate with epochs for the proposed model.

Stochastic gradient descent and the cross-entropy loss function are used in conjunction with deep octonion networks to train the final model. The Nesterov Momentum is set to 0.9 during descent to improve stability and speed convergence. Different learning rates are utilized in each network's epoch to improve network stability. To begin with, the learning rate is set at 0.01; it rises by a factor of 10 for the next 40 evaluations. Rather than training for 200 epochs, deep octonion networks are trained for only 120 epochs since their convergence speed is fast.

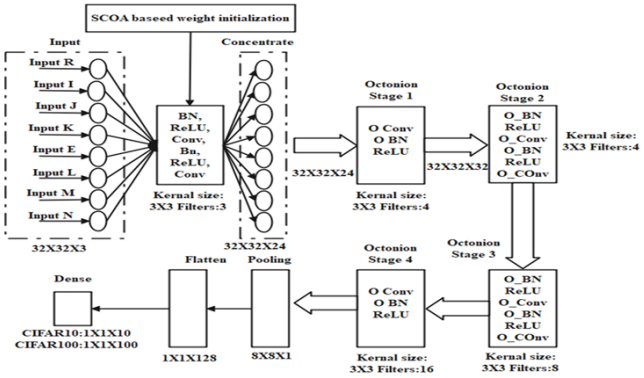

Fig 1. A proposed architecture model

Table 2. The learning rate (%) of octonion CNN

Learning-rate	Epoch
0.1	(20, 60)
0.01	(0, 20)
0.01	(60, 80)
0.001	(80,110)
0.0001	(110, 120)

Fig 2. Sample Collected images and Sample dataset images

2 Results and Discussion

Kersaf is used on a PC running Ubuntu 16.04 with a CPU running at 3.40 GHz clock speed and 64 GB of RAM, and two NVIDIA GeForce GTX1080-Ti graphics cards.

The performance of the classification algorithms was compared according to the criteria of accuracy, precision, and F-score represented in equations (17-20). In the equations, the male is defined as A, the male but predicted as female is considered as B, and the female but identified as male is denoted as C. Finally, the female is correctly identified as female and is represented as D.

$$Accuracy\ (AC) = \frac{A+B}{A+B+C+D} \tag{17}$$

$$Precision\ (P) = \frac{A}{A+B} \tag{18}$$

$$Sensitivity\ (S) = \frac{A}{A+D} \tag{19}$$

$$F-Measure\ (F-M) = \frac{2*Precision*Sensitivity}{Precision+Sensitivity} \tag{20}$$

Here the proposed model is validated by considering two different data ratios i.e. 70% Train- 30% Test and 60% Train- 40% Test. To validate our approach we consider various network models (i.e. LeNet, AlexNet, DenseNet and HDSON) as most of the researchers have used these networks to identify the gender. From the test analysis it has been observed that the accuracy of the proposed model achieved 98.84%, HDSON, LeNet, AlexNet and DenseNet achieved 96.51%, 90.71%, 93.69% and 95.71% respectively for 70%-30%, and the for 60%-40% the proposed model achieved 96.76 % whereas HDSON, LeNet, AlexNet and DenseNet achieved94.93 %, 89.57%, 91.49% and 93.76% respectively. The reason for the better performance of proposed model is that it used both the properties of HDSON and BAM. Therefore, the accuracy is improved for the recognition of gender using facial images. Similarly, in the analysis of S and p, the proposed model achieved 92% & 96% respectively, whereas the LeNet, AlexNet, DenseNet and HDSON achieved 86.67& 84.82%, 89.63% & 85.89%, 91.12% &89.5% and 91.01 % & 89.8 % respectively for different training and testing datasets. Furthermore, when the techniques were tested with F-Measure, the proposed model achieved 90% to 94% for 70:30. The same model achieved 89 % to 91% for 60:40. However, the HDSON achieved highest among all others i.e.91% for 70:30 and has 90.74% for 60:40.

This research proposes a new architecture to determine a person's sex by combining the features of HDSON and BAM. Here we employed octonion orthogonal matching pursuit technique to provide an alternate minimization-based approach for the octonion sparse coding issue which is the expansion of the previous research and developed deep octonion networks (DONs). The OVNN model optimizes the octonion weight initialization by using ReLU as the activation function. As a result, the suggested algorithm is successful because it employed the AR data set, which contains photographs of faces captured by mobile phones from various angles and showed a wide range of emotions belonging to people of both sexes. According to the experimental analysis, the suggested approach provides rapid training with many pictures and obtained high classification accuracy.

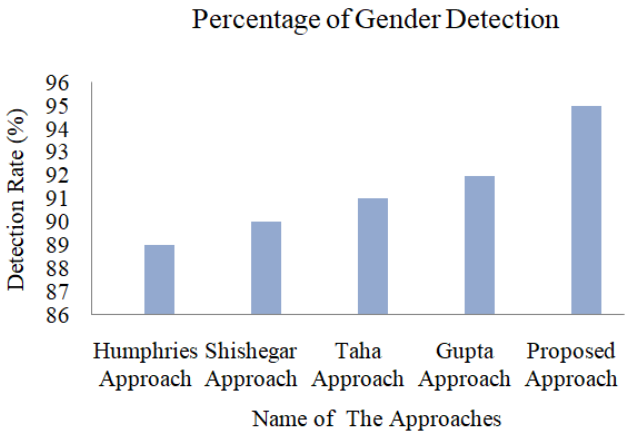

Fig 3. The comparative analysis of approaches

Figure 3 represents the comparative analysis of Humphries (2020)[20], Shishegar (2021)[15], Taha (2022)[8]and Gupta (2023)[7] to distinguish the detection rate of the gender and has been monitored that the proposed approach identifies a greater number of genders among all the existing approaches. Moreover, from obtained statistical data it has been studied that the proposed approach improves the performance of the probability of gender detection by considering precision, accuracy, sensitivity and$F-Measure$.

3 Conclusion

The proposed approach improves the performance of gender detection 3%, as it combines the features of HDSON and BAM. The loss of extracted image is also being reduced, since proposed approach provides the qualitative properties of HADSON and BAM, hence acquired enhanced stored capability which sequentially minimizes the loss of image. Also, it integrates the qualities of HDSON and BAM to optimize time, storage, accuracy, sensitivity and precision of the extracted image. Moreover, the proposed algorithm is simple to operate, so provides the base to signal and image processing researchers to precede the work on this era. The proposed algorithm can be used in paramilitary forces to improve the security against opponents, even if they change their facial activity. Furthermore, the approach can be used to detect the missed persons and helps the local police in real time applications.

References

1) Scheuerman MK, Paul JM, Brubaker JR. How computers see gender: An evaluation of gender classification in commercial facial analysis services. *Proceedings of the ACM on Human-Computer Interaction*. 2019;3:1–33. Available from: https://doi.org/10.1145/3359246.
2) Wu W, Protopapas P, Yang Z, Michalatos P. Gender Classification and Bias Mitigation in Facial Images. *12th ACM Conference on Web Science*. 2020;p. 106–114. Available from: https://doi.org/10.1145/3394231.3397900.
3) Ramalakshmik TJ, Jebaseeli, Venkatesan R. Prediction of Gender from Facial Image Using Deep Learning Techniques. *Journal of Mechanics of Continua and Mathematical Sciences*. 2021;15(2). Available from: https://doi.org/10.26782/jmcms.2020.02.00010.
4) Rasheed J, Waziry S, Alsubai S, Abu-Mahfouz AM. An Intelligent Gender Classification System in the Era of Pandemic Chaos with Veiled Faces. *Processes*. 2022;10(7):1427. Available from: https://doi.org/10.3390/pr10071427.
5) Smith P, Chen C. Transfer Learning with Deep CNNs for Gender Recognition and Age Estimation. *2018 IEEE International Conference on Big Data (Big Data)*. 2018;p. 2564–2571. Available from: https://doi.org/10.1109/BigData.2018.8621891.
6) Lee JHH, Chan YMM, Chen TYY, Chen CSY. Joint Estimation of Age and Gender from Unconstrained Face Images Using Lightweight Multi-Task CNN for Mobile Applications. *2018 IEEE Conference on Multimedia Information Processing and Retrieval (MIPR)*. 2018. Available from: https://doi.org/10.1109/MIPR.2018.00036.
7) Gupta SK, Nain N. Review: Single attribute and multi attribute facial gender and age estimation. *Multimedia Tools and Applications*. 2023;82(1):1289–1311. Available from: https://doi.org/10.1007/s11042-022-12678-6.
8) Taha AM, Zarandah QM, Abu-Nasser BS, Alkayyali ZK, Abu-Naser SS. Gender Prediction from Retinal Fundus Using Deep Learning. *International Journal of Academic Information Systems Research*. 2022;(5):6. Available from: https://philarchive.org/archive/TAHGPF.
9) Di R. Image Classification Using Network Inception- Architecture & Applications. *International Journal of Innovative Research in Science Engineering and Technology*. 2021;10:329–333. Available from: https://doi.org/10.15680/IJIRSET.2021.1001055.
10) Moumen T, El-Melegy AT, Kamal. Linear Regression Classification in the Quaternion and Reduced Biquaternion Domains. *IEEE Signal Processing Letters*. 2022;29:469–473. Available from: https://doi.org/10.1109/LSP.2022.3140682.
11) Islam MM, Baek JH. Deep Learning Based Real Age and Gender Estimation from Unconstrained Face Image towards Smart Store Customer Relationship Management. *Applied Sciences*;11(10):4549. Available from: https://doi.org/10.3390/app11104549.
12) Alonso-Fernandez F, Hernandez-Diaz K, Ramis S, Perales FJ, Bigun J. Facial masks and soft-biometrics: Leveraging face recognition CNNs for age and gender prediction on mobile ocular images. *IET Biometrics*. 2021;10(5):562–580. Available from: https://doi.org/10.1049/bme2.12046.
13) C D, N NU, Maddikunta PKR, Gadekallu TR, Iwendi C, Wei C, et al. Identification of malnutrition and prediction of BMI from facial images using real-time image processing and machine learning. *IET Image Process*. 2022;16:647–658. Available from: https://doi.org/10.1049/ipr2.12222.
14) Katna R, Kalsi K, Gupta S, Yadav D, Yadav AK. Machine learning based approaches for age and gender prediction from tweets. *Multimedia Tools and Applications*. 2022;81(19):27799–27817. Available from: https://doi.org/10.1007/s11042-022-12920-1.
15) Shishegar S, Ghorbani R, Saoud LS, Duchesne S, Pelletier G. Rainfall-runoff modelling using octonion-valued neural networks. *Hydrological Sciences Journal*. 2021;(13):1857–1865. Available from: https://doi.org/10.1007/s11042-022-12920-1.
16) Jose JA, Kumar CS, Sureshkumar S. Region-Based Split Octonion Networks with Channel Attention Module for Tuna Classification. *International Journal of Pattern Recognition and Artificial Intelligence*. 2022;36(07):2250030. Available from: https://doi.org/10.1142/S0218001422500306.
17) Chouhan SS, Kumar R, Sarkar S, Das S. Multistability analysis of octonion-valued neural networks with time-varying delays. *Information Sciences*. 2022;609:1412–1434. Available from: https://doi.org/10.1016/j.ins.2022.07.123.
18) Xiao J, Guo X, Li Y, Wen S, Shi K, Tang Y. Extended analysis on the global Mittag-Leffler synchronization problem for fractional-order octonion-valued BAM neural networks. *Neural Networks*. 2022;154:491–507. Available from: https://doi.org/10.1016/j.neunet.2022.07.031.
19) Kandasamy U, Rajan R. Hopf bifurcation of a fractional-order octonion-valued neural networks with time delays. *Discrete & Continuous Dynamical Systems - S*. 2020;13(9):2537–2559. Available from: https://doi.org/10.3934/dcdss.2020137.
20) Humphries U, Rajchakit G, Kaewmesri P, Chanthorn P, Sriraman R, Samidurai R, et al. Global Stability Analysis of Fractional-Order Quaternion-Valued Bidirectional Associative Memory Neural Networks. *Mathematics*. 2020;8(5):801. Available from: https://doi.org/10.3390/math8050801.
21) Saoud LS, Al-Marzouqi H. Metacognitive Sedenion-Valued Neural Network and its Learning Algorithm. *IEEE Access*. 2020;8:144823–144838. Available from: https://doi.org/10.1109/ACCESS.2020.3014690.
22) Aimeur K, Saoud LS, Ghorbani R. Short-Term Solar Irradiance Forecasting and Photovoltaic System Management Using Octonion Neural Networks. *Applied Solar Energy*. 2020;56(3):219–226. Available from: https://doi.org/10.3103/S0003701X20030020.